Organic & Biomolecular Chemistry

Chemical synthesis of Shiga toxin subunit B using a next-generation traceless "helping hand" solubilizing tag

Journal:	*Organic & Biomolecular Chemistry*
Manuscript ID	OB-ART-09-2019-002012.R2
Article Type:	Paper
Date Submitted by the Author:	15-Nov-2019
Complete List of Authors:	Fulcher, James; University of Utah, Biochemistry Petersen, Mark; University of Utah, Biochemistry Giesler, Riley; University of Utah, Biochemistry Cruz, Zachary; University of Utah, Biochemistry Eckert, Debra; University of Utah, Biochemistry Francis, J. Nicholas; Navigen Pharmaceuticals, Kawamoto, Eric; Navigen Pharmaceuticals, Jacobsen, Michael; University of Utah; Navigen Inc Kay, Michael; University of Utah, Biochemistry

Title

Chemical synthesis of Shiga toxin subunit B using a next-generation traceless "helping hand" solubilizing tag

Authors

James M Fulcher[a,c]

Mark E Petersen[a,d]

Riley J Giesler[a]

Zachary S Cruz[a]

Debra M Eckert[a]

J Nicholas Francis[b,e]

Eric M Kawamoto[b]

Michael T Jacobsen[a,b]

Michael S Kay[a,*]

Affiliations

[a]Department of Biochemistry, University of Utah School of Medicine, Salt Lake City, UT, USA

[b]Navigen Pharmaceuticals, Salt Lake City, UT, USA

[c]Current address: Biological Sciences Division, Pacific Northwest National Laboratory, Richland, WA, USA

[d]Current address: Zymeworks, Vancouver, British Columbia, Canada

[e]Current address: BioFire Diagnostics, Salt Lake City, UT, USA.

* Corresponding author email: kay@biochem.utah.edu (M.S.K.)

†Electronic supplementary information (ESI) available: See DOI: XXXXXXX

Abstract

The application of solid-phase peptide synthesis and native chemical ligation in chemical protein synthesis (CPS) has enabled access to synthetic proteins that cannot be produced recombinantly, such as site-specific post-translationally modified or mirror-image proteins (D-proteins). However, CPS is commonly hampered by aggregation and insolubility of peptide segments and assembly intermediates. Installation of a solubilizing tag consisting of basic Lys or Arg amino acids can overcome these issues. Through the introduction of a traceless cleavable linker, the solubilizing tag can be selectively removed to generate native peptide. Here we describe the synthesis of a next-generation amine-reactive linker *N*-Fmoc-2-(7-amino-1-hydroxyheptylidene)-5,5-dimethylcyclohexane-1,3-dione (Fmoc-Ddap-OH) that can be used to selectively introduce semi-permanent solubilizing tags ("helping hands") onto Lys side chains of difficult peptides. This linker has improved stability compared to its predecessor, a property that can increase yields for multi-step syntheses with longer handling times. We also introduce a new linker cleavage protocol using hydroxylamine that greatly accelerates removal of the linker. The utility of this linker in CPS was demonstrated by the preparation of the synthetically challenging Shiga toxin subunit B (StxB) protein. This robust and easy-to-use linker is a valuable addition to the CPS toolbox for the production of challenging synthetic proteins.

Introduction

Total chemical synthesis of proteins enables techniques such as racemic protein crystallography[1] and mirror-image phage display,[2] as well as structure/function studies of post-translationally modified proteins.[3, 4] Through the use of solid-phase peptide synthesis (SPPS)[5] and native chemical ligation (NCL),[6-8] chemical protein synthesis (CPS)[9, 10] permits the routine synthesis of proteins up to ~200 amino acids. However, challenges with peptide insolubility are commonly encountered during the assembly of synthetic proteins and can limit the scope of CPS.[11] Ambitious synthesis projects are often hampered by peptide segments that are too insoluble to be purified by HPLC or dissolved at the high concentrations needed for efficient NCL.[12, 13]

To address and overcome issues encountered with insoluble peptides, several groups have devised strategies that incorporate two main components: 1) a solubilizing tag composed of multiple basic amino acids, and 2) a linker between the tag and peptide that can be removed to restore the native peptide sequence. For example, work by Kent[14] and Aimoto[15] detailed a thioester linker combined with a poly-Arg tag to increase the solubility of hydrophobic peptide segments. After HPLC purification, this tag can be removed through transthioesterification during NCL. Although this direct thioester linker is restricted to Boc-SPPS, several Fmoc-compatible strategies have been developed.[16-18] The main disadvantage to these strategies is that they cannot survive more than one NCL reaction.[19] Recently, several NCL-compatible strategies introducing semi-permanent solubilizing tags have been presented. Liu's group developed a salicylaldehyde-derived linker and Arg-tag for the introduction of solubilizing removable backbone modifications (RBMs), which have the advantage of not requiring specific residues or side chains for implementation.[20, 21] Several Cys-based linkers/solubilizing tags have also been developed recently including the phenylactamidomethyl (Phacm) linker by Brik's group, the Arg-tagged ACM^R by Danishefsky's group, and an Arg-tagged trityl linker from the Yoshiya group.[22-26] Additionally, the Yoshiya group recently introduced a self-cleavable canaline linker.[27]

The introduction of these linkers and solubilizing tags has expanded the scope of CPS, but significant barriers to their broader use remain. These barriers include complex

linker synthesis, limited availability of sites for attachment of linkers, or lability under certain reaction conditions. Building on previous work with the Dde protecting group,[28-30] we recently described a linker (*N*-Fmoc-1-(4,4-dimethyl-2,6-dioxocyclo-hexylidene)-3-[2-(2-aminoethoxy)ethoxy]-propan-1-ol or Fmoc-Ddae-OH) that aimed to address these limitations with its ease of use and compatibility with common conditions employed during Fmoc-SPPS and NCL.[31] The Ddae linker could easily be incorporated at various Lys sites within a peptide and tracelessly removed to generate the target of interest. This Ddae linker met all of our initial design requirements; however, we sought to improve its stability and handling properties, as well as reduce the cost of synthesis to increase its utility and accessibility.

Here we describe the synthesis of a next generation linker, Fmoc-Ddap-OH (*N*-Fmoc-2-(7-amino-1-hydroxyheptylidene)-5,5-dimethylcyclohexane-1,3-dione), that has increased stability in aqueous solvents and is an easy-to-handle powder compared to Ddae. Incorporation of the Ddap linker follows the same protocol as Ddae and is achieved through direct addition onto a free amine, typically a Lys side chain, present on an otherwise protected peptide (Scheme 1). Following Fmoc removal, the solubilizing sequence can be built through standard Fmoc-SPPS. After cleavage using TFA-containing standard scavengers, the Ddap linker is stable to several commonly used buffers in chemical protein synthesis. Once the handling steps that require enhanced solubilization are complete, the linker can be cleaved using an α-nucleophile, such as hydrazine or hydroxylamine.[32] We demonstrate the versatility of this new linker in the synthetically challenging Shiga toxin subunit B (StxB), a 69-amino acid protein essential for the pathogenesis of *Shigella* and Shiga Toxin-Producing *E. coli* (STEC).[33] Synthetic StxB and a recombinant StxB control were compared using high-resolution mass spectrometry (HRMS), circular dichroism (CD), size exclusion chromatography (SEC) and analytical ultracentrifugation (AUC) to validate the synthetic approach.

Results and Discussion

Synthesis and Characterization of Linkers using the Model Peptide C20

We began by substituting the PEG_2 moiety present in our original Ddae linker with 6, 7, or 8-carbon alkyl chains (termed Ddax, Ddap, and Ddac, respectively; Fig. 1 and S1-16) as the starting materials are commercially available and relatively inexpensive (Table S1). After flash purification and lyophilization, we observed that the Ddap and Ddac linkers are solids at room temperature, unlike the Ddax and Ddae linkers, which are viscous oils (Fig. S17). These linkers were then compared throughout several stages of SPPS assembly using the model peptide C20 (Ac-DWTKNITD**K(Dde)**IDQIIHDFVDK-NH_2, Fig. S18). This model peptide was selected due to its diverse peptide sequence (including a Lys residue), high crude purity (>70%), and previous use in the characterization of the Ddae linker.[31] After synthesis of C20 at 30 μmol scale, the Dde group was removed using 5% hydrazine in DMF to reveal an unprotected primary amine at Lys9. The coupling (attachment of the linker to amine) was performed by adding 1 mL of 200 mM linker in N-methylpyrrolidine (NMP) to the resin at 37°C. Attachment of alkyl chain linkers reached completion in <15 min compared to 60 min required for Ddae coupling (Fig. S19). As no other additives are needed for coupling, the excess linker can be recycled by flash chromatography and reused. After coupling of the linkers, we performed standard Fmoc-SPPS to build a Lys_6 solubilizing tag (referred to as a "helping hand" or HH) for each C20 linker variant. We chose six Lys residues based on previous reports describing the benefits of positively charged residues in addressing insolubility.[34, 35] All peptides were cleaved from solid supports using standard TFA cleavage conditions (95% TFA, 2.5% TIS, 2.5% H_2O) and purified by RP-HPLC (Fig. S20-23).

With these purified peptides in hand, we next tested the cleavage kinetics of each linker using 1 M hydrazine in denaturing buffer (6 M GnHCl, 100 mM $NaPO_4$, pH 7.5) with C20(HH) peptides at 0.5 mM. Timepoints were analyzed using analytical HPLC monitoring at 214 nm, and product formation was calculated based on relative peak areas with a correction factor to account for the UV absorbance of the cleaved linker (Fig. S24 and S25). All alkyl chain linkers were cleaved within 8 h, compared to 4 h for the PEG_2-based Ddae

linker (Fig. 2A). Comparison of C20 with Lys_6-Ddap and Lys_6-Ddae in several common reaction conditions used in CPS demonstrates the improved stability of the Ddap linker over Ddae as well (Table 1 and Fig. S26). Although cleavage kinetics are similar between the alkyl chain linkers, we picked the Ddap linker as the most favorable compound due to its lower-cost starting material compared to Ddac and solid physical state compared to Ddax. Therefore, we continued our characterization using the Ddap linker as our lead candidate.

Ddap Cleavage Kinetics Using Hydroxylamine

The greater stability of Ddap, though advantageous for minimizing dissociation during multiple handling steps, led us to wonder if the cleavage time could be reduced by using a different α-nucleophile. Considering the pKa of the conjugate acid of hydroxylamine (~6) allows for a higher proportion of nucleophilic species at lower pH than hydrazine (pKa ~8),[36] we rationalized that hydroxylamine at pH 6.75 could potentially be much faster than our standard hydrazine cleavage conditions (1 M hydrazine in denaturing buffer: 6 M GnHCl, 100 mM $NaPO_4$, pH 7.5).[32] The lower pH of 6.75 was chosen to more closely match NCL conditions and reduce the potential for hydroxylamine-induced cleavage of peptide bonds.[37] The rate of cleavage with 1 M hydroxylamine at pH 6.75 in denaturing buffer was ~19x faster than our previous cleavage protocol using 1 M hydrazine at pH 7.5 (k of 224.8 vs. 11.6 x 10^{-3} s^{-1}), reaching completion within 30 min (Fig. 2B and S27). The reaction also proceeded cleanly without formation of any significant side products (Fig. 2C and Fig. S28-29). We extended both cleavage reactions for 24 h to investigate the potential for side reactions. Under these exceptionally harsh conditions, the majority of the C20 peptide remained unmodified by LC-MS, however several hydrazide and hydroxamate modifications were observed (Fig. S30 and S31).[38]

UV Absorbance of Ddap linker

One characteristic of the Ddap linker we observed in our initial characterization was significant 280 nm absorbance (A_{280}). As A_{280} from Trp or Tyr residues is a convenient method for determining peptide concentration, we determined the molar extinction coefficient (ε, $M^{-1}{\cdot}cm^{-1}$) of our linker so that it could be utilized as a UV tag and would not interfere with peptide concentration measurements. Utilizing our C20 test peptide modified with an N-terminal carboxyfluorescein, we compared the A_{280} of the peptide with or without the Ddap linker at equal concentrations as determined using the A_{495} of fluorescein (Fig. S32 and S33).[39] The difference in A_{280} was found to correspond to an ε of ~14,600 $M^{-1} \cdot cm^{-1}$ in denaturing buffer (6 M GnHCl, 200 mM $NaPO_4$, pH 8). It is worth noting the ε of Ddap is considerably higher than Trp and Tyr, which have ε of 5,500 and 1,490 $M^{-1} \cdot cm^{-1}$, respectively.[40] Therefore, this property of Ddap would be particularly useful for peptides lacking Tyr or Trp, allowing it to be used as a tag for UV monitoring or concentration measurements via A_{280}.

Synthesis of Shiga Toxin Subunit B using the Helping Hand

We tested the utility of our next-generation helping hand by incorporating it into the synthesis of Shiga toxin subunit B (StxB; note StxB contains an N-terminal signal peptide that is cleaved to form the mature protein, Fig. 3A).[41] Our initial synthesis attempts to make the full-length 69-amino acid mature protein via SPPS were hampered by poor crude quality and insolubility in HPLC conditions. To improve the quality of the crude peptide produced by SPPS, StxB was divided into two segments (StxB-N and StxB-C) for NCL, and several pseudoproline dipeptides were used in the synthesis of StxB-N.[42, 43] To address insolubility of StxB-N, we installed the Ddap helping hand at Lys47 (Fig. 3B and 3C). StxB represents a good test for our new linker as it not only displays insolubility in aqueous conditions but also contains an Asn-Gly in its sequence, a reported hydroxylamine cleavage site (though under much harsher conditions such as 2 M hydroxylamine at pH 9).[37, 44, 45]

StxB-N was synthesized as a C-terminal hydrazide for NCL.[46-48] The C-terminal hydrazide was utilized as a thioester surrogate due to its convenience and compatibility with Fmoc-SPPS. StxB-N was prepared with Boc- protection at the N-terminus and an orthogonally protected Lys(Dde) for incorporation of the helping hand (Fig. 3B). As a

control to evaluate improvement in solubility, StxB-N was also produced without a solubilizing tag. StxB-C was synthesized with a C-terminal acid using standard Fmoc-SPPS. The crude peptides (StxB-N and StxB-N(HH)) were dissolved in HPLC buffer (20% ACN 0.1% TFA) until saturation and centrifuged at 5,000g for 20 min, and the supernatants were lyophilized to determine the soluble peptide fraction. StxB-N without the solubilizing tag was only soluble to 0.4 mg/mL and was not studied further, while StxB-N(HH) with the solubilizing tag was 40-fold more soluble (16.0 mg/mL). This increased solubility considerably sharpened the analytical HPLC trace (Fig. 4). Although the HPLC purification of StxB-N(HH) was considerably easier with the helping hand due to the improved solubility, we could not resolve material containing a Val deletion (-99 Da) from the correct product. StxB-C was purified without issues using HPLC. With the purified peptides in hand (Fig. S34 and S35), we proceeded with NCL. StxB-N(HH) (0.5 mM) was converted in situ to an MPAA thioester and combined with 3 equiv. of StxB-C (1.5 mM) in denaturing buffer. NCL between StxB-N(HH) and StxB-C was complete within 30 min, with minimal loss of product due to hydrolysis of StxB-N(HH) (Fig. 5 and S36). Cleavage of the helping hand was performed in one pot by equal volume addition of 2 M hydroxylamine, pH 6.75 in denaturing buffer. As anticipated, cleavage proceeded rapidly and was complete within 30 min, producing full-length StxB after a final HPLC purification (Fig. 5 and S37).

Importantly, we did not observe any side products resulting from cleavage at the Asn-Gly bond in StxB, suggesting that treatment with 1 M hydroxylamine is relatively mild. A final step-wise dialysis under oxidizing conditions was performed to allow for disulfide bond formation followed by folding of the synthetic material. The deletion products that carried over from the initial, challenging HPLC purification of StxB-N(HH) did not did not appear to fold correctly and were not found in the final, post-dialysis clarified material (Fig. 6A and S38). After folding, synthetic StxB was compared to a recombinant StxB control using high-resolution mass spectrometry (HRMS), circular dichroism (CD), size-exclusion chromatography (SEC), and analytical ultracentrifugation (AUC). Comparison of data between the recombinant and synthetic StxB from all four techniques closely agree, suggesting similar chemical structure (mass spectra in Fig. 6A), secondary structure (CD

spectra in Fig. 6B), and the expected pentameric quaternary structure (SEC in Fig. 6C and AUC in ESI Fig. S39).

Conclusions

In this study, we describe the one-step synthesis of a next-generation amine-reactive linker, Fmoc-Ddap-OH, using inexpensive and accessible starting materials. Like the first-generation Fmoc-Ddae-OH, this linker can be used to address insolubility of peptides containing a Lys residue through the semi-permanent addition of basic Lys/Arg amino acids (referred to as "helping hands"). An added convenience is that this new linker is a solid powder at room temperature unlike the previous viscous oil. We also found the alkyl chain linker conferred two-fold greater stability in various common reaction conditions used in the assembly of synthetic proteins. For large protein syntheses that require a solubilizing tag and have numerous handling steps, the greater stability of this linker in aqueous conditions should prevent helping hand leakage and provide higher final yields. The greater stability may be conferred by lower electrophilicity of the carbon undergoing nucleophilic attack due to differences in inductive effect for each linker. Substitution of the inductively withdrawing alkoxy group in Ddae for the inductively donating alkyl group in Ddax/Ddap/Ddac may reduce the electrophilicity and therefore vulnerability of the dimedone ring to nucleophilic attack. The ^{13}C NMR data for the linkers support this, as the carbon undergoing nucleophilic substitution shows a trend of deshielding with Ddae<Ddax<Ddap<Ddac[49] (Fig. S4, S8, S12, and S16). Therefore, design of more stable linkers could be accomplished with longer alkyl chains or addition of electron-donating groups to the dimedone ring itself. This added stability, though advantageous for multiple handling steps, increased the time needed to cleave the Ddap linker using hydrazine. To this end, we demonstrated a new method for cleaving the linker with hydroxylamine that greatly accelerated the rate of cleavage, allowing complete removal of the linker within 30 min. We expect these accelerated cleavage conditions to be particularly advantageous for removal of multiple Ddap linkers from a single peptide or protein.

The synthesis of StxB not only presents an ideal opportunity to test the new Ddap linker in a challenging real-world CPS problem, but also results in a relevant target for mirror-image phage display (MIPD).[2] Shiga toxins (Stx), classical AB5 toxins, are produced by various Shigella bacterial species and are important virulence factors in the development of hemorrhagic colitis/shigellosis.[33, 50] StxB mediates the introduction of the ribotoxic StxA by binding to host glycosphingolipid Gb3.[33] Currently there are no approved treatments for the prevention or reduction of disease symptoms, and treatment with traditional antibiotics can increase the risk of developing the potentially fatal hemolytic uremic syndrome.[51] A D-peptide therapeutic identified using MIPD that blocks the interaction of StxB with Gb3 directly at the site of binding would be of substantial clinical benefit. A requirement for MIPD, however, is the synthesis of the target in the opposite (D-) chirality. With a synthesis strategy for L-StxB now established, synthesis of the mirror-image D-StxB can be performed following the same steps described here. In conclusion, this convenient Ddap linker with solubilizing Lys_6 tag is a widely accessible and easy-to-use tool that enables the synthesis of insoluble peptides and proteins.

Conflicts of Interest

DME and MSK are consultants and equity holders in Navigen, Inc., which is developing D-peptide drugs.

Acknowledgments

The authors would like to thank Dr. Paul Sebahar, Nai-Pin Lin, Patrick Erickson, and Judah Evangelista for experimental/material assistance. We also thank Dr. Sandra Osburn-Staker of the Proteomics Core Facility (University of Utah) for high-resolution mass spectrometry analysis and Dr. Vincent Aucagne for his helpful discussions.

References

1. T. O. Yeates and S. B. H. Kent, *Annual Review of Biophysics*, 2012, **41**, 41-61.
2. T. N. M. Schumacher, L. M. Mayr, D. L. Minor, M. A. Milhollen, M. W. Burgess and P. S. Kim, *Science*, 1996, **271**, 1854-1857.
3. M. Jbara, H. Sun, G. Kamnesky and A. Brik, *Current Opinion in Chemical Biology*, 2018, **45**, 18-26.
4. M. Nawatha, J. M. Rogers, S. M. Bonn, I. Livneh, B. Lemma, S. M. Mali, G. B. Vamisetti, H. Sun, B. Bercovich, Y. Huang, A. Ciechanover, D. Fushman, H. Suga and A. Brik, *Nat Chem*, 2019, **11**, 644-652.
5. R. B. Merrifield, *Journal of the American Chemical Society*, 1963, **85**, 2149-2154.
6. P. E. Dawson, T. W. Muir, I. Clark-Lewis and S. Kent, *Science*, 1994, **266**, 776-779.
7. T. M. Hackeng, J. H. Griffin and P. E. Dawson, *Proceedings of the National Academy of Sciences of the United States of America*, 1999, **96**, 10068-10073.
8. S. B. H. Kent, *Chemical Society Reviews*, 2009, **38**, 338-351.
9. S. Kent, *Bioorganic and Medicinal Chemistry*, 2017, **25**, 4926-4937.
10. S. B. H. Kent, *Protein Science*, 2019, **28**, 313-328.
11. M. Paradís-Bas, J. Tulla-Puche and F. Albericio, *Chemical Society Reviews*, 2016, **45**, 631-654.
12. L. R. Malins and R. J. Payne, *Current opinion in chemical biology*, 2014, **22**, 70-78.
13. F. Saito, H. Noda and J. W. Bode, *ACS Chemical Biology*, 2015, **10**, 1026-1033.
14. E. C. B. Johnson and S. B. H. Kent, *Tetrahedron letters*, 2007, **48**, 1795-1799.
15. T. Sato, Y. Saito and S. Aimoto, *Journal of Peptide Science*, 2005, **11**, 410-416.
16. A. C. Baumruck, D. Tietze, L. K. Steinacker and A. A. Tietze, *Chemical Science*, 2018, **9**, 2365-2375.
17. J. B. Blanco-Canosa and P. E. Dawson, *Angewandte Chemie - International Edition*, 2008, **47**, 6851-6855.
18. J.-X. Wang, G.-M. Fang, Y. He, D.-L. Qu, M. Yu, Z.-Y. Hong and L. Liu, *Angewandte Chemie International Edition*, 2015, **54**, 2194-2198.
19. X. Li, T. Kawakami and S. Aimoto, *Tetrahedron Letters*, 1998, **39**, 8669-8672.
20. J.-B. B. Li, S. Tang, J.-S. S. Zheng, C.-L. L. Tian and L. Liu, *Accounts of Chemical Research*, 2017, **50**, 1143-1153.
21. J.-S. S. Zheng, Y. He, C. Zuo, X.-Y. Y. Cai, S. Tang, Z. A. Wang, L.-H. H. Zhang, C.-L. L. Tian and L. Liu, *Journal of the American Chemical Society*, 2016, **138**, 3553-3561.
22. S. Tsuda, M. Mochizuki, H. Ishiba, K. Yoshizawa-Kumagaye, H. Nishio, S. Oishi and T. Yoshiya, *Angewandte Chemie*, 2018, **130**, 2127-2131.
23. S. Tsuda, S. Masuda and T. Yoshiya, *Organic & Biomolecular Chemistry*, 2019, **17**, 1202-1205.
24. J. A. Brailsford, J. L. Stockdill, A. J. Axelrod, M. T. Peterson, P. A. Vadola, E. V. Johnston and S. J. Danishefsky, *Tetrahedron*, 2018, **74**, 1951-1956.
25. S. Bondalapati, E. Eid, S. M. Mali, C. Wolberger and A. Brik, *Chemical Science*, 2017, **8**, 4027-4034.
26. S. K. Maity, G. Mann, M. Jbara, S. Laps, G. Kamnesky and A. Brik, *Organic Letters*, 2016, **18**, 3026-3029.
27. S. Tsuda, H. Nishio and T. Yoshiya, *Chemical Communications*, 2018, **54**, 8861-8864.
28. B. W. Bycroft, W. C. Chan, S. R. Chhabra and N. D. Hone, *Journal of the Chemical Society, Chemical Communications*, 1993, 778-779.
29. S. RamáChhabra, *Journal of the Chemical Society, Chemical Communications*, 1993, 776-777.
30. B. Kellam, W. C. Chan, S. R. Chhabra and B. W. Bycroft, *Tetrahedron Letters*, 1997, **38**, 5391-5394.

31. M. T. Jacobsen, M. E. Petersen, X. Ye, M. Galibert, G. H. Lorimer, V. Aucagne and M. S. Kay, *Journal of the American Chemical Society*, 2016, **138**, 11775-11782.
32. J. J. Díaz-Mochón, L. Bialy and M. Bradley, *Organic Letters*, 2004, **6**, 1127-1129.
33. A. R. Melton-Celsa, *Microbiology Spectrum*, 2014, **2**, 1-21.
34. A. Kato, K. Maki, T. Ebina, K. Kuwajima, K. Soda and Y. Kuroda, *Biopolymers*, 2007, **85**, 12-18.
35. M. A. Khan, M. M. Islam and Y. Kuroda, *Biochim Biophys Acta*, 2013, **1834**, 2107-2115.
36. F. E. Condon, R. T. Reece, D. G. Shapiro, D. C. Thakkar and T. B. Goldstein, *Journal of the Chemical Society, Perkin Transactions 2*, 1974, DOI: 10.1039/p29740001112, 1112-1121.
37. R. J. Simpson, 2004, DOI: 10.1021/pr040022a, pp. 343-424.
38. M. Antorini, U. Breme, P. Caccia, C. Grassi, S. Lebrun, G. Orsini, G. Taylor, B. Valsasina, E. Marengo, R. Todeschini, C. Andersson, P. Gellerfors and J.-G. Gustafsson, *Protein Expression and Purification*, 1997, **11**, 135-147.
39. M. C. Mota, P. Carvalho, J. Ramalho and E. Leite, *International Ophthalmology*, 1991, **15**, 321-326.
40. C. N. Pace, F. Vajdos, L. Fee, G. Grimsley and T. Gray, *Protein science : a publication of the Protein Society*, 1995, **4**, 2411-2423.
41. N. G. Seidah, A. Donohue-Rolfe, C. Lazure, F. Auclair, G. T. Keusch and M. Chrétien, *Journal of Biological Chemistry*, 1986, **261**, 13928-13931.
42. T. Wöhr and M. Mutter, *Tetrahedron Letters*, 1995, **36**, 3847-3848.
43. T. Wöhr, F. Wahl, A. Nefzi, B. Rohwedder, T. Sato, X. Sun, M. Mutter and C. Lausanne, *Journal of the American Chemical Society*, 1996, **118**, 9218-9227.
44. P. Bornstein and G. Balian, *Methods in Enzymology*, 1977, **47**, 132-145.
45. D. L. Crimmins, S. M. Mische and N. D. Denslow, 2005, DOI: 10.1002/0471140864.ps1104s40.
46. G.-M. M. Fang, Y.-M. M. Li, F. Shen, Y.-c. C. Huang, J.-B. B. Li, Y. Lin, H.-k. K. Cui and L. Liu, *Angewandte Chemie International Edition*, 2011, **50**, 7645-7649.
47. J.-S. Zheng, S. Tang, Y.-K. Qi, Z.-P. Wang and L. Liu, *Nature Protocols*, 2013, **8**, 2483-2495.
48. J. S. Zheng, S. Tang, Y. Guo, H. N. Chang and L. Liu, *ChemBioChem*, 2012, **13**, 542-546.
49. S. Bolvig, F. Duus and P. E. Hansen, *Magnetic Resonance in Chemistry*, 1998, **36**, 315-324.
50. K. L. Kotloff, M. S. Riddle, J. A. Platts-mills, P. Pavlinac and A. K. M. Zaidi, *The Lancet*, 2017, **391**, 801-812.
51. S. E. Majowicz, E. Scallan, A. Jones-bitton, M. Jan, J. Stapleton, F. J. Angulo, D. H. Yeung and M. D. Kirk, *Food Microbiology*, 2014, **11**, 447-455.

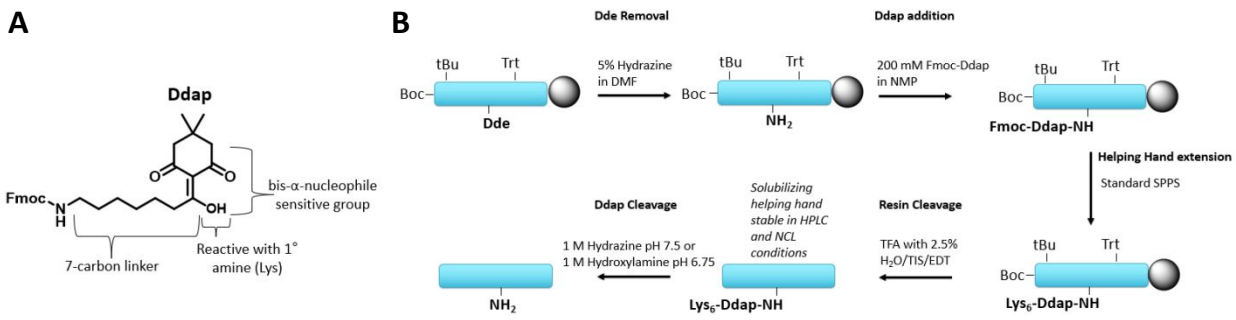

Scheme 1. **(A)** Key properties of the Ddap linker and **(B)** steps for the installation/removal of a semipermanent solubilizing helping hand.

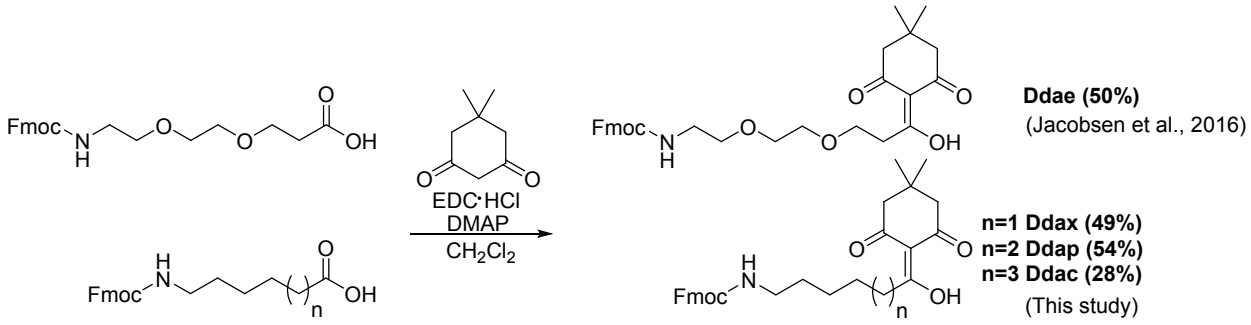

Fig. 1. One-step synthetic route for all linkers used in this study (yields shown next to each linker). See ESI for synthesis details.

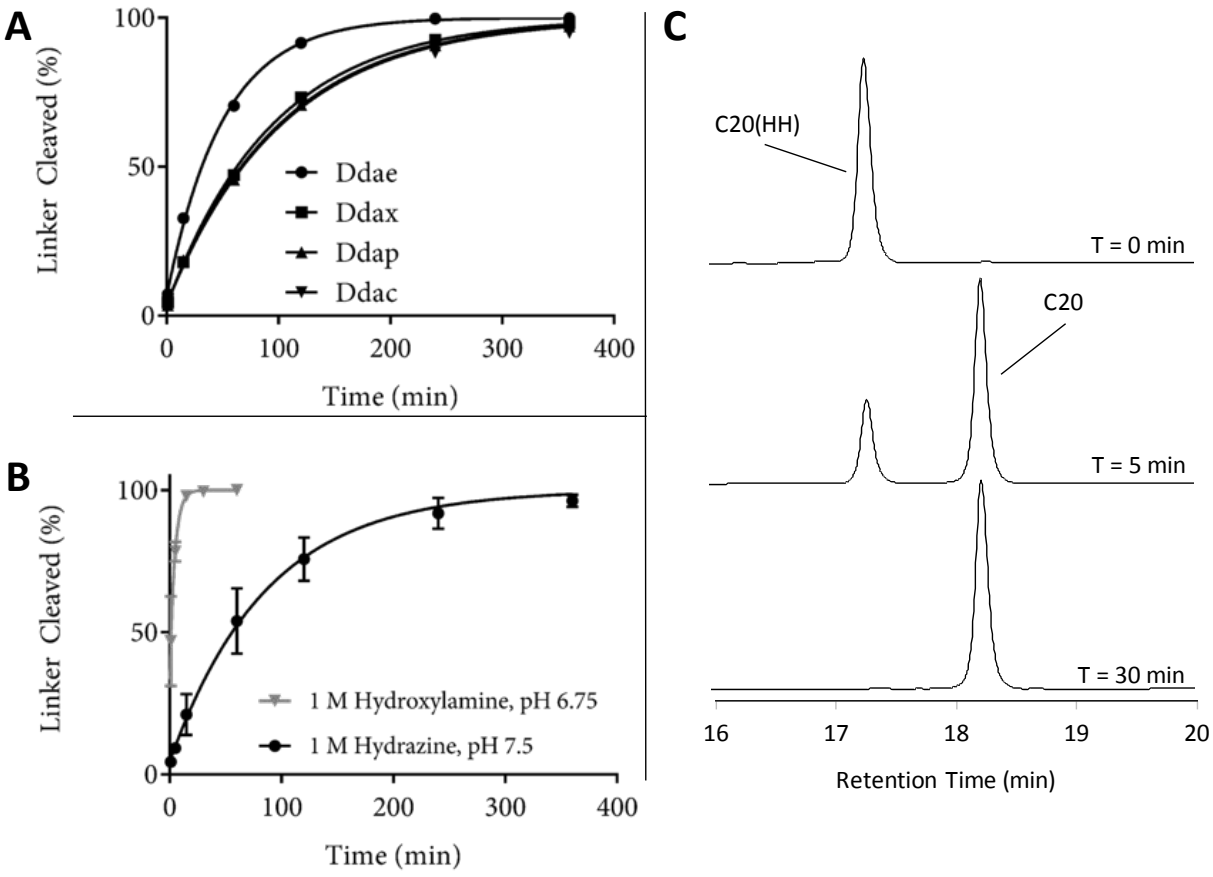

Fig. 2. Characterization of linker cleavage kinetics with different α-nucleophiles.
(A) Cleavage kinetics of C20(HH) with all linkers using 1 M hydrazine in cleavage buffer (6 M GnHCl, 100 mM $NaPO_4$, pH 7.5). **(B)** Cleavage kinetics of C20(Lys_6-Ddap) with 1 M hydrazine or hydroxylamine in cleavage buffer at pH 6.75 vs. 7.5. Average of 2 replicates shown with s.d. error bars. **(C)** Representative HPLC traces of C20(Lys_6-Ddap) cleavage using 1 M hydroxylamine in cleavage buffer, pH 6.75. Y-axis shows A_{214} normalized to the highest peak.

A

```
        30          40          50          60
TPDCVTGKVE  YTKYNDDDTF  TVKVGDKELF  TNRWNLQSLL
        70          80
LSAQITGMTV  TIKTNACHNG  GGFSEVIFR
```

B

[StxB-N(HH)]:
Boc-TPDCVTGKVEYTKYNDD**DT**FTVKVGDK(KKKKKK-Ddap)EL**FT**NRWNLQSLL**LS**AQITGMT**VT**IKTNA-$NHNH_2$

[StxB-C]:
CHNGGGFSEVIFR-OH

C

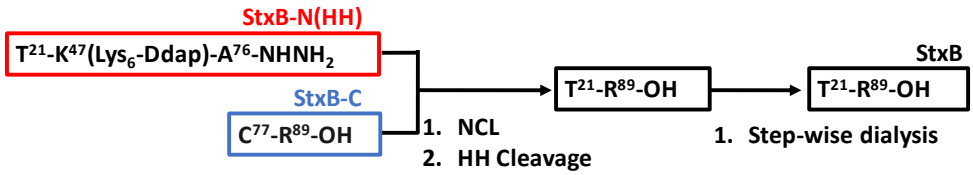

Fig. 3. StxB sequence and synthesis strategy.
(A) Sequence of mature StxB (without precursor signal peptide). N-terminal (T^{21} – A^{76}) and C-terminal (C^{77} – R^{89}) segments are shown in red and blue, respectively. **(B)** Sequences of individual peptides showing position of pseudoproline dipeptides (black), helping hand (underline), and Boc-modified N-terminus. **(C)** Assembly strategy for the two segments showing one-pot NCL/helping hand cleavage to produce full-length StxB before folding through step-wise dialysis under oxidizing conditions.

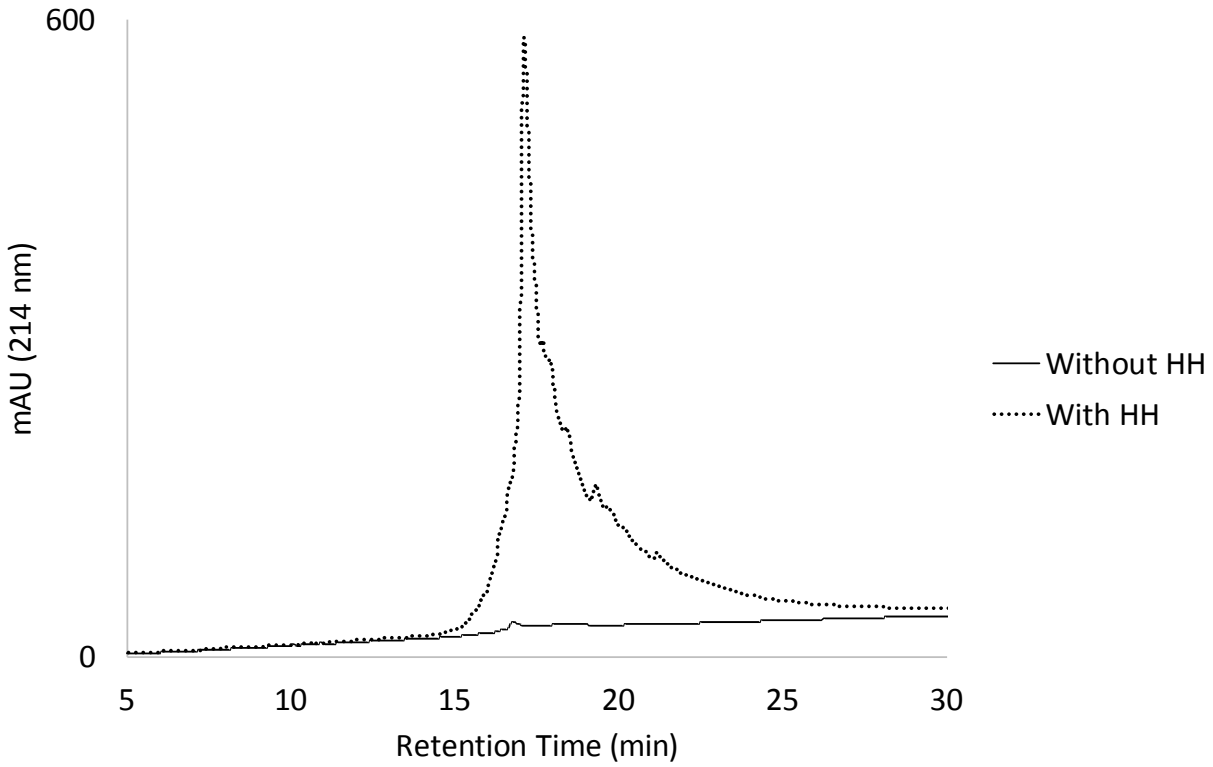

Fig. 4. Comparison of crude StxB-N with and without helping hand. StxB-N and StxB-N(HH) were dissolved in HPLC buffer (20% B, 80% A) until saturation before centrifugation at 5,000g for 20 min to remove precipitated material. HPLC traces were collected for StxB-N and StxB-N(HH) with a linear gradient of 10-60% B over 30 min.

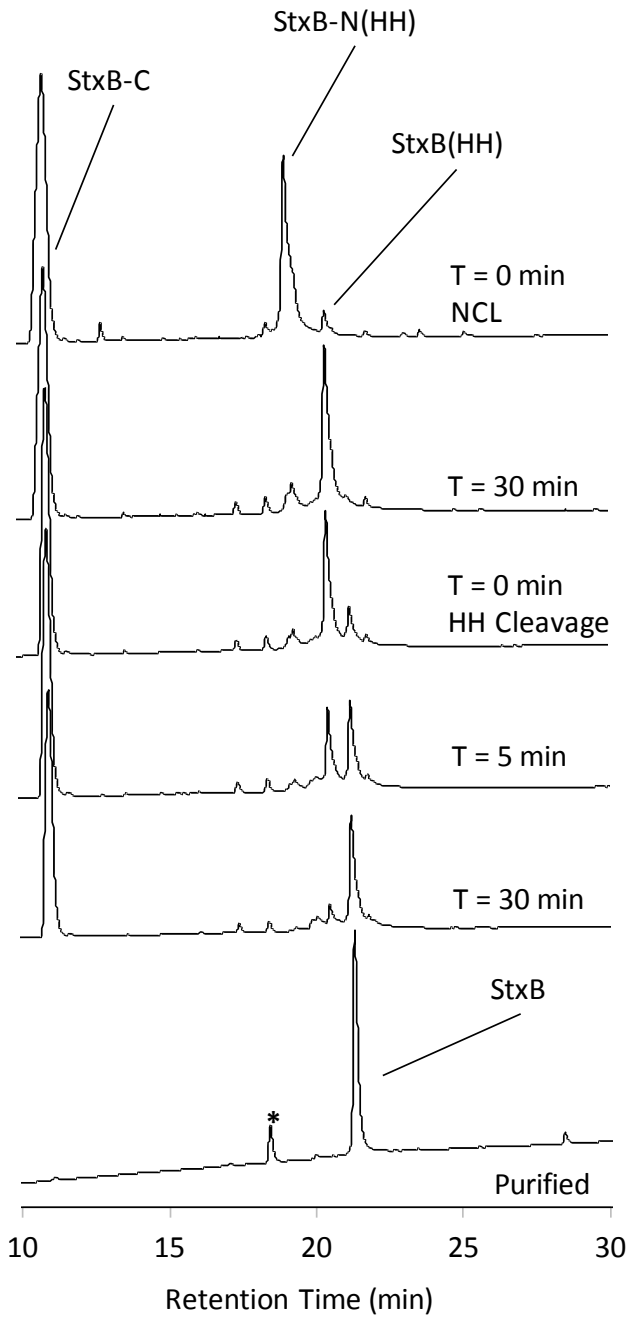

Fig. 5. StxB assembly.
HPLC traces demonstrating NCL between StxB-C and StxB-N(HH) before one-pot cleavage of the helping hand using 1 M hydroxylamine (pH 6.75) to produce full-length StxB. Y-axis is A_{214} and the gradient was 10 to 60% B. * indicates oxidized-MPAA contaminant that coeluted with full-length StxB during final HPLC purification.

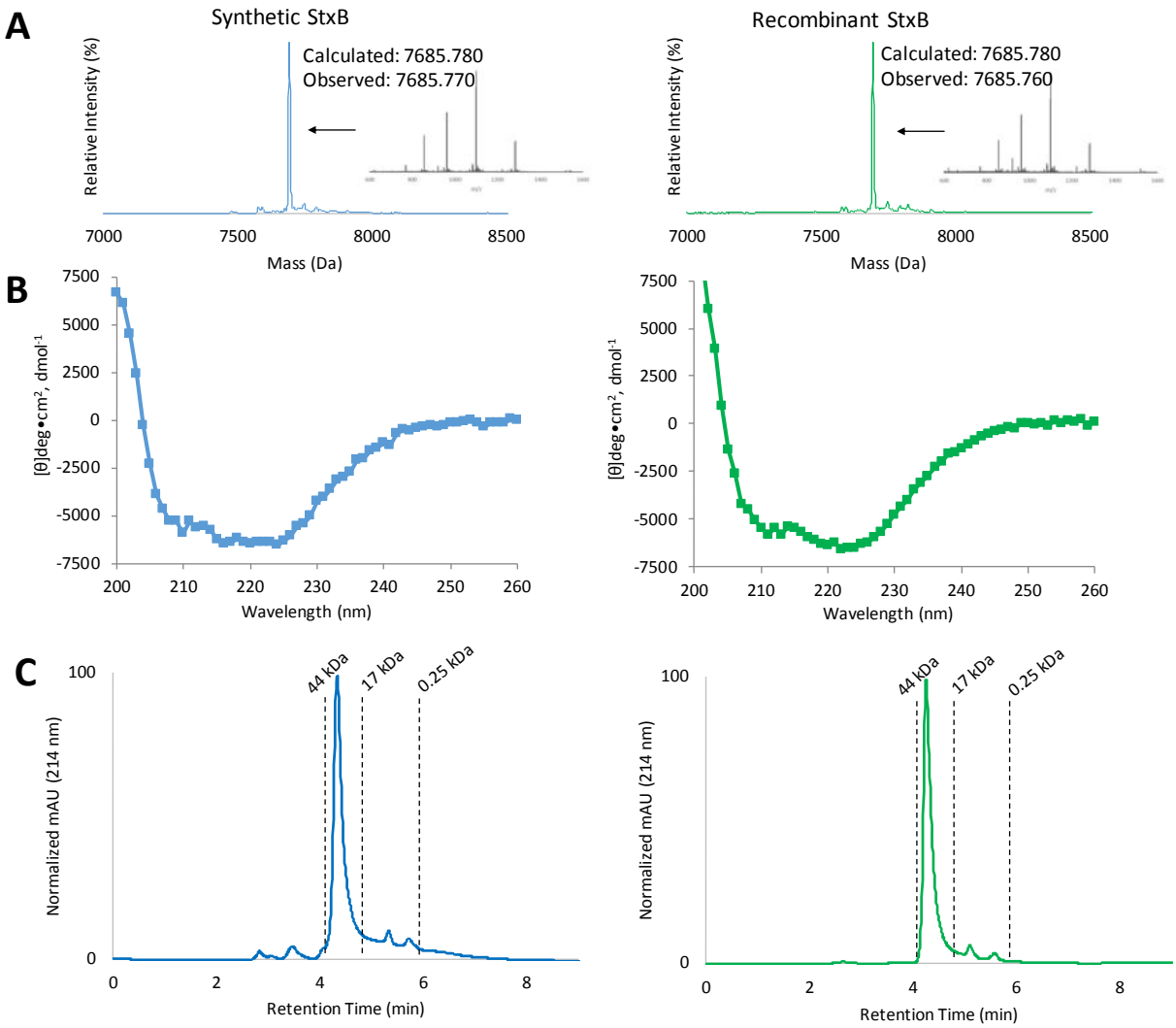

Fig. 6. Characterization of recombinant and synthetic StxB. Comparison of synthetic (blue) and recombinant StxB (green). **(A)** High-resolution mass spectrometry shows matching masses. **(B)** Circular dichroism spectra indicate matching secondary structure. **(C)** Size-exclusion chromatography suggests both synthetic and recombinant StxB form a pentamer.

Buffer	C20(Lys_6-Ddae) Uncleaved Linker (%) after 48 h	C20(Lys_6-Ddap) Uncleaved Linker (%) after 48 h
0.1% TFA in 50% ACN (HPLC Buffer)	90	95
6 M GnHCl, 100 mM $NaPO_4$, pH 3	88	90
6 M GnHCl, 200 mM $NaPO_4$, pH 7	89	92
6 M GnHCl, 5% AcOH	89	94
6 M GnHCl, 100 mM $NaPO_4$, 200 mM $MeONH_2$, pH 3 (Thz cleavage buffer)	60	87
6 M GnHCl, 200 mM $NaPO_4$, 200 mM MPAA, 50 mM TCEP, pH 7 (NCL conditions)	86	94

Table 1. Stability comparison between C20(Lys_6-Ddae) and C20(Lys_6-Ddap) after 48 h in several commonly used buffers in CPS. See ESI for experimental details.